# Heterodimeric Capping Protein from *Arabidopsis* Is Regulated by Phosphatidic Acid

## Shanjin Huang,* Lisa Gao,* Laurent Blanchoin,† and Christopher J. Staiger*

*Department of Biological Sciences and The Bindley Bioscience Center, Purdue University, West Lafayette, IN 47907-2064; and †Laboratoire de Physiologie Cellulaire Végétale, Commissariat à l'Energie Atomique/Centre National de la Recherche Scientifique/Université Joseph Fourier, F38054 Grenoble, France

The cytoskeleton is a key regulator of morphogenesis, sexual reproduction, and cellular responses to extracellular stimuli. Changes in the cellular architecture are often assumed to require actin-binding proteins as stimulus-response modulators, because many of these proteins are regulated directly by binding to intracellular second messengers or signaling phospholipids. Phosphatidic acid (PA) is gaining widespread acceptance as a major, abundant phospholipid in plants that is required for pollen tube tip growth and mediates responses to osmotic stress, wounding, and phytohormones; however, the number of identified effectors of PA is rather limited. Here we demonstrate that exogenous PA application leads to significant increases in filamentous actin levels in *Arabidopsis* suspension cells and poppy pollen grains. To investigate further these lipid-induced changes in polymer levels, we analyzed the properties of a key regulator of actin filament polymerization, the heterodimeric capping protein from *Arabidopsis thaliana* (AtCP). AtCP binds to PA with a $K_d$ value of 17 $\mu$M and stoichiometry of ~1:2. It also binds well to PtdIns(4,5)P$_2$, but not to several other phosphoinositide or acidic phospholipids. The interaction with PA inhibited the actin-binding activity of CP. In the presence of PA, CP is unable to block the barbed or rapidly growing and shrinking end of actin filaments. Precapped filament barbed ends can also be uncapped by addition of PA, allowing rapid filament assembly from an actin monomer pool that is buffered with profilin. The findings support a model in which the inhibition of CP activity in cells by elevated PA results in the stimulation of actin polymerization from a large pool of profilin–actin. Such regulation may be important for the response of plant cells to extracellular stimuli as well as for the normal process of pollen tube tip growth.

## INTRODUCTION

Membrane phospholipids are key regulators of cellular signaling responses and reorganization of the cytoplasmic architecture in all eukaryotic cells. Although much early work in this arena focused on the role of polyphosphoinositide (PPI) turnover, there is growing evidence for the function of other acidic phospholipids as signaling intermediates. In particular, phosphatidic acid (PA) and lysophospholipids are implicated in diverse signaling cascades (Meijer and Munnik, 2003; Wang, 2004; Testerink and Munnik, 2005). PA is generated through two major pathways: hydrolysis of the structural lipid phosphatidylcholine by phospholipase D (PLD) enzymes, and phosphorylation of the lipid second messenger diacylglycerol (DAG) by DAG kinase (Meijer and Munnik, 2003; Wang, 2004; Testerink and Munnik, 2005). In animal cells, actin cytoskeleton polymerization is stimulated by PA (Ha and Exton, 1993; Ha *et al.*, 1994; Zhou *et al.*, 1995; Siddiqui and English, 1997; Shin *et al.*, 1999), and both PA and PLD activity have been implicated in multiple stress signaling responses of plant cells (Meijer and Munnik, 2003; Wang, 2004).

Transient increases in cellular PA in response to a variety of stresses have been measured for different plant cells.

These include responses to fungal elicitors and bacterial nodulation factors, the phytohormone abscisic acid, osmotic and cold stresses, and wounding (reviewed in Meijer and Munnik, 2003; Wang, 2004; Testerink and Munnik, 2005). Many of these stress responses correlate with rapid and dramatic changes in actin cytoskeleton organization (Staiger, 2000; Drøbak *et al.*, 2004). For example, in response to attack by fungal pathogens or elicitor, epidermal cells accumulate a unique actin array at the site of penetration (Kobayashi *et al.*, 1992, 1994; Gross *et al.*, 1993). In another case, *Vicia* and bean root hairs respond to lipochito-oligosaccharide Nod factors produced by *Rhizobium* spp. with a transient depolymerization of the actin cytoskeleton followed by formation of a new actin cytoskeletal array that coordinates the resumption of tip growth (Cárdenas *et al.*, 1998; Miller *et al.*, 1999). Several effectors of PA signaling have been identified, including protein kinases and phosphatases, lipid kinases, ion channels, and NADPH oxidase, but their role in these particular stress responses remains ambiguous (Meijer and Munnik, 2003; Anthony *et al.*, 2004; Testerink *et al.*, 2004; Zhang *et al.*, 2004). A recent study by Lee *et al.* (2003) showed that exogenous application of PA to soybean suspension-culture cells resulted in a substantial increase in actin filament levels, presumably functioning through a calcium-dependent protein kinase.

PA and PLD activity are also implicated in the actin-dependent tip growth of root hairs and pollen tubes (Ohashi *et al.*, 2003; Potocký *et al.*, 2003; Samaj *et al.*, 2004; Monteiro *et al.*, 2005a). Reducing the normally high cellular levels of PA with 1-butanol treatment inhibits pollen germination and tip

growth (Potocký *et al.,* 2003; Monteiro *et al.,* 2005a). This reduction correlates with dissipation of the tip-focused $Ca^{2+}$ gradient, loss of secretory vesicles from the apical region, and enhanced bundling and disorganization of the actin filaments (Monteiro *et al.,* 2005a). Increasing cellular PA by the exogenous application of lipid stimulates pollen germination and alleviates the effects of 1-butanol (Potocký *et al.,* 2003; Monteiro *et al.,* 2005a). It has also been reported that excess PA stimulates an increase in actin filaments at the tip region of pollen tubes (Monteiro *et al.,* 2005b). Because germination and tip growth depend on precise regulation, organization, and dynamics of the actin cytoskeleton (Gibbon *et al.,* 1999; Vidali *et al.,* 2001), actin and its associated proteins are likely cellular targets and sensors of fluctuations in PA levels.

The function of the actin cytoskeleton is coordinated by more than 70 classes of actin-binding protein (ABP). Many of these have been documented as stimulus-response elements, coordinating fluxes through PPI pools into reorganization of the cytoskeleton and concomitant changes in cellular architecture or motility. Many ABPs have been characterized for the ability to bind PtdIns$(4,5)P_2$, but there is growing evidence for binding to and regulation by 3-phosphorylated PPIs (Yin and Janmey, 2003). Only one ABP appears to be strongly regulated by other phospholipids; human gelsolin binds to lysoPA and its filament severing and barbed-end capping activities are inhibited by this biologically active lipid (Meerschaert *et al.,* 1998). Gelsolin is not, however, regulated by PA (Meerschaert *et al.,* 1998), nor is profilin (Lassing and Lindberg, 1985), $\alpha$-actinin (Fraley *et al.,* 2003), or chicken CapZ (Schafer *et al.,* 1996). Several plant ABPs have been isolated and characterized (Staiger and Hussey, 2004), and some are also regulated by PtdIns$(4,5)P_2$, including profilin (Drøbak *et al.,* 1994), ADF/cofilin (Gungabissoon *et al.,* 1998), and capping protein (CP; Huang *et al.,* 1998).

Here, we report that *Arabidopsis thaliana* CP, a heterodimeric capping protein that binds to the barbed ends of actin filaments (Huang *et al.,* 2003), is regulated by a moderate affinity interaction with PA. To our knowledge, this is the first evidence for the marked regulation of any eukaryotic ABP by this particular phospholipid. The biological significance of this finding is given further credibility because of the high levels of endogenous PA found in plant cell membranes (Dorne *et al.,* 1988; Zonia and Munnik, 2004; Li *et al.,* 2004). With kinetic analyses of pyrene-actin assembly and disassembly, we demonstrate that binding to PA inhibits the nucleation and barbed-end capping activity of CP. These results were confirmed by the analysis of single actin filaments with fluorescence microscopy. We propose a model whereby PA modulates actin cytoskeleton organization in plant cells. Specifically, increased cellular PA is predicted to stimulate the uncapping of filament barbed ends, leading to the extension of actin filaments from a large pool of profilin–actin subunits. Indeed, we verify that exogenous PA treatment of pollen and suspension cells leads to a significant increase in actin filament levels. Our model could explain the behavior of actin cytoskeletal arrays observed during several plant stress responses and during normal extension of pollen tubes by tip growth.

## MATERIALS AND METHODS

### Phospholipid Preparation

The following phospholipids were purchased from Sigma-Aldrich (St. Louis, MO): 1,2-diacyl-*sn*-glycero-3-phosphate from egg yolk (P9511, PA); 1,2-diacyl-*sn*-glycero-3-phospho-(1-D-myo-inositol) (P5766, PtdIns); 1,2-diacyl-*sn*-glycero-3-phospho-(1-D-myo-inositol 4,5-bisphosphate) (P9763, PtdIns$(4,5)P_2$); 1-oleoyl-*sn*-glycerol 3-phosphate (L7260, LPA), and phosphatidylserine (PS). All PPIs used in this study were dipalmitoyl derivatives. Phospholipids were dissolved in chloroform and the solvent was evaporated under a stream of $N_2$. After addition of water, the mixture was allowed to sit for 5 min and then was dispersed by sonication in a water bath for 5 min to form micelles or multilamellar vesicles, which were stored on ice before use.

### Growth of Arabidopsis Suspension Cell Cultures and Poppy Pollen Germination

An *A. thaliana* Columbia-0 suspension cell culture was obtained from Nick Carpita (Purdue University) and maintained by subculturing weekly into 50 ml of culture medium containing 3.2 g/l Gamborg-B5 with minimal organics (Sigma), 2% (wt/vol) sucrose, 1.1 mg/ml 2,4-D, and 10 mM 2-(*N*-morpholino)-ethanesulfonic acid (MES), pH 5.7. Cultures were grown in Erlenmeyer flasks at room temperature, under ambient light, with constant shaking (115-rpm rotation). After 3–4 d of subculture, cells were used for PA treatments. Germination of *Papaver rhoeas* (field poppy) pollen (generously provided by Noni Franklin-Tong, University of Birmingham, United Kingdom) was performed according to Snowman *et al.* (2002). The counting of germination rate was performed according to Gibbon *et al.,* (1999). After 1 h of growth, any protrusion from the germination aperture was scored as positive for germination. At least 200 pollen grains were counted for each treatment and experiments were repeated three times.

### Imaging of Actin Filaments and Fluorescent PA

The internalization of exogenously supplied PA was examined according to Potocký *et al.* (2003) with the addition of 1 $\mu$M BODIPY-PA (D-3805; Molecular Probes, Eugene, OR) into pollen germination medium. Images were collected with a Bio-Rad MRC 1024 confocal laser scanning microscope (Bio-Rad, Hercules, CA) equipped with a 60$\times$ 1.4 NA PlanApo objective (Nikon, Melville, NY). Images were acquired from near the medial plane of each cell, 0.5-$\mu$m optical sections were scanned and captured, and three Kalman-filtered scans were averaged for each optical section.

Pollen grains were stained with Alexa-488-phalloidin (Molecular Probes) as described by Snowman *et al.* (2002). Microscopy was performed on the laser scanning confocal platform described above. The fluorescent phalloidin was excited with the 488-nm line of a Kr/Ar laser, 0.5-$\mu$m optical sections were scanned and captured, and three Kalman-filtered scans were averaged for each optical section. Images were prepared by projections of 40 optical sections through an individual pollen grain. For the colocalization of actin filaments and BODIPY-PA, pollen tubes were fixed and stained with rhodamine-phalloidin as described above, after incubating with 1 uM BODIPY-PA for 1 h in germination medium. Images were acquired by spinning disk confocal microscopy with a 100$\times$ 1.4 NA PlanApo objective mounted on a Nikon T200 stand. Illumination through the Yokogawa spinning disk unit (CSU10B; Yokogawa Electronics Co., Tokyo, Japan) was generated by a Coherent Innova 70c mixed gas laser (Prairie Technologies, Middleton, WI) with lines at 488 nm and 568 nm provided by an acoustic-optical tuned filter. Single optical sections were collected with a Photometrics Coolsnap HQ CCD camera (Roper Scientific, Tucson, AZ) driven by MetaMorph 6.1 software (Universal Imaging, Downington, PA).

To analyze the pixel intensity of individual pollen grains, pollen was observed by epifluorescence illumination under a wide-field fluorescence microscope (Nikon E600) equipped with a 60$\times$ 1.4 NA PlanApo objective. The digital images of pollen grains were collected with a Hamamatsu Orca-100 CCD camera (Hamamatsu Photonics, Bridgewater, NJ) and were processed and analyzed with Metamorph software.

### Quantification of Filamentous Actin

The measurement of actin filament levels in poppy pollen grains treated with different phospholipids for 80 min was according to the method of Gibbon *et al.* (1999), as modified by Snowman *et al.* (2002). For actin filament quantification of *Arabidopsis* suspension cells, the method was based on that for pollen with the following modifications: A 1-ml volume of *Arabidopsis* suspension cell was treated with various concentrations of PA or with PS as a phospholipid control. After incubation with phospholipids for 2 h, cells were stabilized and fixed by the addition of 300 $\mu$M 3-maleimidobenzoyl-*N*-hydroxysuccinimide ester (MBS; Sigma), and NP-40 was added to a final concentration 0.05%. The cells were washed three times with TBST (50 mM Tris-HCl, pH 7.5, 200 mM NaCl, 0.05% NP-40) and neutralized in TBST containing 1 mM DTT. After extensive washing, the suspension cells were incubated with 2 $\mu$M Alexa-488-phalloidin and 5 $\mu$M ethidium bromide (EB) overnight. Actin filament levels were determined by eluting bound phalloidin from cells with methanol, and the resulting solution analyzed by spectrofluorometry with excitation at 492 nm and emission at 514 nm. The cell number was estimated by measuring the eluted EB with excitation and emission wavelengths of 513 and 615 nm. The relative actin filament content was defined by phalloidin fluorescence divided by EB fluorescence.

### Protein Purification

Recombinant *A. thaliana* capping protein (AtCP) was purified from *Escherichia coli* as described previously (Huang *et al.,* 2003). Actin was isolated from

rabbit skeletal muscle acetone powder, and monomeric Ca-ATP-actin was purified by Sephacryl S-300 chromatography (Kouyama and Mihashi, 1981; as modified by Pollard, 1984) in Buffer G (5 mM Tris-HCl, pH 8, 0.2 mM ATP, 0.1 mM CaCl$_2$, 0.5 mM DTT, 0.1 mM azide). Actin was labeled on Cys-374 with pyrene iodoacetamide (Pollard, 1984). Mouse capping protein (MmCP; α1β2 heterodimer) was kindly provided by D. R. Kovar (Yale University).

### Phospholipid Binding

The interaction of CP with acidic phospholipids was tested by protein–lipid blot overlays according to the methods of Dowler *et al.* (1999). Commercially available PIP-strips (P-6001; Echelon Biosciences, Salt Lake City, UT) were blocked in a solution of 3% (wt/vol) fatty acid free BSA (Sigma; A-3803) in TBST for 1 h at room temperature. The blocking solution was supplemented with 5 μg/ml (83 nM) of purified CP and the membranes incubated overnight at 4°C with agitation. After removing the protein solution and extensive TBST washes, membranes were incubated with 1:1000 polyclonal anti-AtCPA and anti-AtCPB (Huang *et al.*, 2003) followed by 1:100,000 HRP-conjugated anti-rabbit IgG (Sigma). Antibody–protein complexes were visualized by enhanced chemiluminescence (Pierce Supersignal West Pico substrate; Rockford, IL) and exposed to autoradiographic film. Experiments were performed at least three times, and controls for specificity included omitting the actin-binding protein or the primary antibody and use of other plant actin-binding proteins.

### Intrinsic Tryptophan Fluorescence

An equilibrium dissociation constant ($K_d$) for the binding of AtCP and MmCP to phospholipids was determined by measuring the quenching of intrinsic tryptophan fluorescence as described by Lin *et al.* (1997). Fluorescence spectra were recorded at room temperature with an PTI Quantamaster spectrofluorometer (QM-2000-SE; Photon Technology International, South Brunswick, NJ). Briefly, 2 ml of CP solution (100 nM) in 25 mM HEPES, 100 mM KCl, 0.4 mM EGTA, 0.5 mM β-mercaptoethanol, pH 7.5, was placed in a 1-cm$^2$ quartz cuvette and stirred with a mini-magnetic stirrer. After allowing 5 min for equilibration, using excitation at 292 nm, the tryptophan fluorescence emission spectrum (300–400 nm) was recorded. Titration was performed by multiple additions of phospholipids from a stock solution. For PA, the stock solution was 3.6 mM, and additions ranged from 3.6 to 132.1 μM final concentration; for LPA, the stock solution was 4.3 mM, and additions ranged from 4.3 to 159 μM; for PtdIns(4,5)P$_2$, the stock solution was 940 μM, and additions ranged from 0.9 to 34.8 μM. After each addition of micelles, fluorescence was monitored in the spectrofluorometer. Although AtCP contains seven tryptophan residues between the two subunits (Huang *et al.*, 2003), we assumed for purposes of this analysis a simple two-state mechanism of fluorescence change. The affinity of CP for various phospholipids was determined by quenching of CP fluorescence as a function of the concentration of phospholipid using Equation 1:

$$F = F_f + F_b \left( \frac{(K_d + [P] + [CP]) - \sqrt{(K_d + [P] + [CP])^2 - (4[P][CP])}}{2[CP]} \right) \quad (1)$$

where F is the observed fluorescence, $F_f$ the fluorescence of free CP, $F_b$ the fluorescence of AtCP bound to phospholipid, [P] is the total concentration of phospholipid, and [CP] is the total concentration of AtCP. The stoichiometry of binding (ρ) was determined by the method of Stinson and Holbrook (1973):

$$1/(1 - \theta) K_a = [lipid_T]/\theta - \rho[CP_T] \quad (2)$$

where θ is the fractional binding ($\Delta F/\Delta F_{max}$), ρ is the stoichiometry of binding, [lipid$_T$] is the total concentration of phospholipid, and [CP$_T$] is the total capping protein concentration. The fluorescence maximum (F$_{max}$) was estimated by extrapolation of the regression line to the ordinate of double reciprocal plots of fluorescence change (ΔF) versus [phospholipid residues] (Gibbon *et al.*, 1998). When $1/(1 - \theta)$ is plotted against [lipid$_T$]/θ the intercept with the x-axis is ρ [CP$_T$]. ρ can then be calculated by dividing the intercept with CP concentration (Ward, 1985).

### Actin Nucleation Assay

Actin nucleation was carried out essentially as described by Schafer *et al.* (1996). Monomeric actin at 2 μM (5% pyrene labeled) was incubated with 500 nM AtCP for 5 min in Buffer G. To test the effect of phospholipids on nucleation, 500 nM AtCP was preincubated with varying concentrations of phospholipids in Buffer G for 5 min. Fluorescence of pyrene-actin was monitored with the spectrofluorometer after the addition of 1/10 volume of 10× KMEI (1× contains 50 mM KCl, 1 mM MgCl$_2$, 1 mM EGTA, and 10 mM imidazole-HCl, pH 7.0).

### Dynamics of Actin Filament Depolymerization

Filamentous actin at 5 μM (40–50% pyrene labeled) was mixed with 500 nM AtCP, incubated at room temperature for 5 min, and diluted 25-fold into Buffer G (Huang *et al.*, 2003). To test the effect of phospholipids on actin filament depolymerization, 500 nM AtCP was preincubated with varying concentrations of phospholipids in Buffer G for 5 min. The decrease in pyrene fluorescene accompanying actin depolymerization was monitored for 1000 s after dilution.

### Filament Uncapping Assay

The uncapping assay is a modification of the actin elongation assay described previously (Huang *et al.*, 2003). AtCP, 200 nM, was incubated with 0.8 μM preformed actin filaments in KMEI for 5 min at room temperature. The reaction mixtures were supplemented with 1 μM G-actin (5% pyrene labeled), saturated by 4 μM human profilin I to prevent spontaneous nucleation, and various concentrations of phospholipid. Fluorescence of pyrene-actin was monitored with the spectrofluorometer after the addition of the mixture. In the absence of PA, virtually no assembly of new actin filaments was observed during the time course of the assay.

### Determination of Association and Dissociation Rate Constants

We determined rate constants for capping of actin filaments by simulating the time course of actin elongation in the presence of AtCP using the reactions in the model shown below, according to Schafer *et al.* (1996) and Blanchoin and Pollard (2002), where A is the actin monomer bound to profilin, N is the concentration of filaments ends, F is the concentration of actin in filaments, and C is capping protein concentration. We used KINSIM (Barshop *et al.*, 1983) and FITSIM (Zimmerle and Frieden, 1989) to adjust experimental curves to theoretical curves: A + N ⇔ F + N and N + C ⇔ NC.

Three separate experiments were performed roughly according to the elongation assay described by Schafer *et al.*, (1996), and each resulting set of polymerization curves was fit independently with KINSIM and FITSIM. In these reactions, 1.2 μM actin assembled into filaments served as the "seeds" for polymerization from a pool of profilin-bound actin monomers in the presence or absence of different amounts of AtCP. To initiate assembly, seeds were added to a cuvette containing 1 μM monomeric actin (5% pyrene labeled), 4 μM human profilin I, and varying amounts of AtCP prepared in 1× KMEI, and the change in fluorescence was monitored for 1200 s.

### Fluorescence Microscopy of Actin Filaments

Individual actin filaments labeled with fluorescent phalloidin were imaged by fluorescence microscopy as described previously (Huang *et al.*, 2003). To test the effect of phospholipids on actin polymerization, 500 nM AtCP was preincubated with varying amounts of phospholipid micelles. Actin filaments were observed by epi-fluorescence illumination under a Nikon Microphot SA microscope equipped with a 60×, 1.4 NA Planapo objective, and digital images were collected with a Hamamatsu ORCA-ER CCD camera using MetaMorph software.

## RESULTS

### Exogenous PA Treatment Results in Increased Actin Filament Levels in Plant Cells

Recently, Lee *et al.* (2003) found that applying PA to suspension-cultured soybean cells caused a substantial increase in the amount of actin present in the polymer pool. We extended this finding by applying PA at various concentrations to *Arabidopsis* suspension cells and to *P. rhoeas* (field poppy) pollen. It seems likely that PA enters intracellular compartments where it can interact with cytoplasmic proteins, because a substantial amount of BODIPY-labeled PA has been shown to enter pollen tubes with a timecourse of 10–30 min (Potocký *et al.*, 2003). We confirmed this by supplying BODIPY-PA to hydrated poppy pollen and imaging its uptake with fluorescence microscopy (Figure 1). Within minutes of incubation in 1 μM BODIPY-PA, the cytoplasm of *Papaver* pollen grains and pollen tubes became brightly and uniformly fluorescent (unpublished data). After 20–30 min, fluorescent PA was also observed in numerous, large organelles (Figure 1, B and D). Time-lapse imaging revealed that these organelles were motile and required actin filaments for movement, because they were stationary after brief treatments with 1 μM latrunculin B (unpublished data). Colabeling with rhodamine-phalloidin and imaging with spinning disk confocal microscopy shows that the organelles were surrounded by, and sometimes appeared to reside on, the axial network of actin filament cables or bundles (Figure 1E).
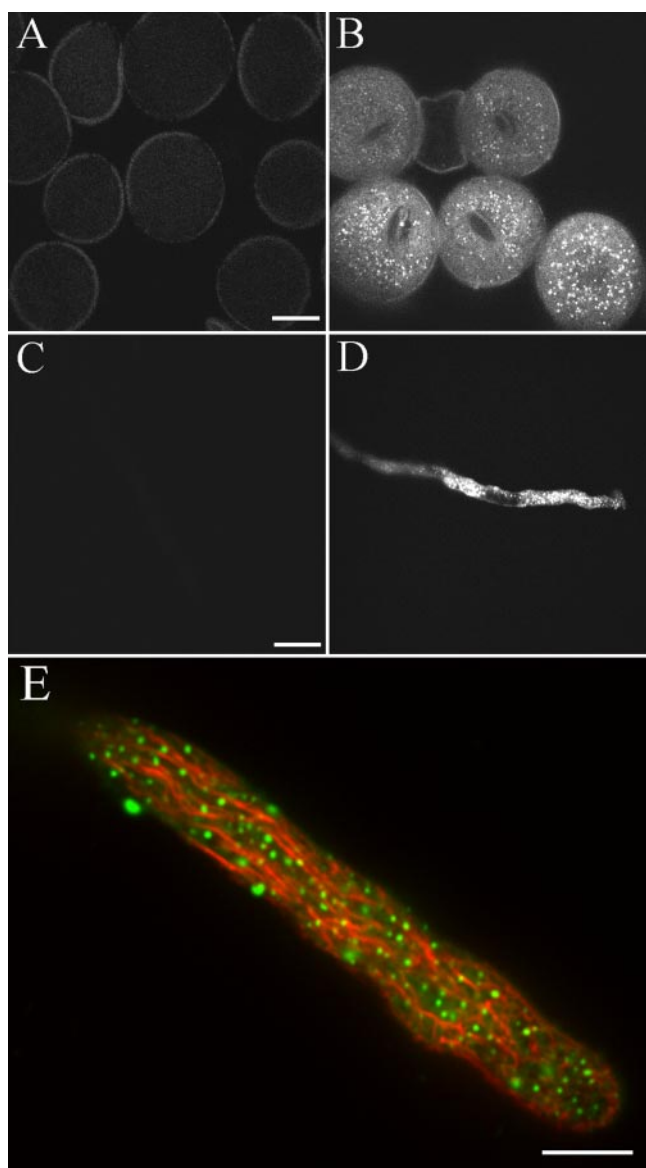
**Figure 1.** Exogenous BODIPY-PA is taken into *Papaver rhoeas* (field poppy) pollen grains and pollen tubes. BODIPY-PA, 1 $\mu$M, was added to the germination medium and incubated for 1 h. Images were acquired by confocal laser scanning microscopy. (A–D) Single optical sections from the medial plane. Bar, (A) 10 $\mu$m for A and B; (C) 20 $\mu$m for C and D. (A) Untreated pollen grain. (B) Pollen grain treated with 1 $\mu$M BODIPY-PA. (C) Untreated pollen tube. (D) Pollen tube treated with 1 $\mu$M BODIPY-PA. (E) Pollen tube labeled with rhodamine phalloidin to stain actin filaments (red) and with BODIPY-PA (green). The two-color image is a a single optical section through a medial plane of the pollen tube, collected by spinning disk confocal microscopy. Bar, 10 $\mu$m.

In populations of PA-treated cells and untreated controls, actin filament levels were analyzed using a quantitative phalloidin-binding assay that has been adapted for use in plant cells (Gibbon *et al.*, 1999; Snowman *et al.*, 2002). As shown in Figure 2, modest treatments with PA (10–100 $\mu$M for <2 h) resulted in 20–40% increases in measurable actin filament levels for both cell types. In both instances, fluorescence levels from control populations without exogenous PA were normalized to 100%. For *Arabidopsis* suspension cells, treatment with 50 and 100 $\mu$M PA resulted in actin

filament levels that were 123 $\pm$ 2 and 115 $\pm$ 6% (mean $\pm$ SD; n = 3) of the control (Figure 2A). These differences are specific because treatment with another acidic phospholipid, PS, had no measurable effect on actin filament levels (98 $\pm$ 4%). The actin filament levels in PA-treated cells were significantly different from the PS-treated cells (Student's *t* test, p < 0.02). As shown in Figure 2B, poppy pollen grains also showed elevated actin filament levels in response to PA. Treatments with 25, 50, and 100 $\mu$M PA gave levels (mean $\pm$ SD; n = 3) that were 134 $\pm$ 12, 125 $\pm$ 8, and 109 $\pm$ 4% of the control without lipid treatment. Again, all of these actin filament levels were significantly different (p < 0.03) from the PS-treated controls, which had a mean value of 96 $\pm$ 8%. Additionally, the closely related lipid, lyso-PA (LPA) had no significant effect when applied at 25, 50, and 100 $\mu$M (mean values of 93 $\pm$ 14, 85 $\pm$ 21, 84 $\pm$ 21%, respectively). This finding seems to exclude the possibility that increases in filamentous actin are due to LPA that contaminates many commercial preparations of PA. Thus, increases in cellular PA levels can result in net actin polymerization for several types of plant cell. It is noteworthy that the greatest effects on polymeric actin levels were observed with low concentrations of PA. This suggests that there may be multiple cytoskeletal targets for PA action.

The spectrofluorometry results from cell populations were confirmed and extended with fluorescence microscopy of single cells after Alexa-488-phalloidin labeling. Typically, the actin cytoskeleton appeared brighter and somewhat more dense in pollen grains treated with PA (Figure 2C, right image) when compared with those treated with PS (Figure 2C, left image) or untreated (unpublished data). These hydrated and germinating pollen grains have a reticulate network of actin filaments filling the cytoplasm; although PA increases the brightness of these arrays, it does not alter the overall organization. Similar increases in fluorescence level were observed for early bicellular pollen that have an additional cage of actin filaments surrounding the generative cell and vegetative nucleus (unpublished data; see also Snowman *et al.*, 2002). The average fluorescence pixel intensity of individual grains was 1561 $\pm$ 26 (n = 140) and 1615 $\pm$ 31 (n = 127) for untreated and PS-treated pollen, respectively (Figure 2D). By contrast, the fluorescence intensity of pollen grains treated with 25 $\mu$M PA had a value of 2343 $\pm$ 37 (n = 165). Because PA treatment appears to elevate actin filament levels in pollen grains, we wanted to know whether this had any effect on germination rate. As shown in Figure 2E, the mean germination rate ($\pm$SD; n = 3) for untreated controls and pollen grains treated with 100 $\mu$M PS was 63.0 $\pm$ 0.8 and 61 $\pm$ 9%, whereas 25, 50, and 100 $\mu$M PA treatments gave values of 68 $\pm$ 6, 64 $\pm$ 6, and 64 $\pm$ 10%, respectively. These results show that exogenous PA caused no significant change in pollen germination frequency. Thus, PA treatment leads to enhanced levels of filamentous actin in poppy pollen grains but does not have a detrimental effect on pollen germination.

The primary alcohol, 1-butanol, can be used as an effective inhibitor of PA signaling through the PLD pathway (Testerink and Munnik, 2005). PLD is able to use primary alcohols rather than water as an acceptor for the phosphatidyl group, leading to the production of phosphatidylbutanol rather than PA. This effectively reduces cellular PA levels in many cells, including pollen (Monteiro *et al.*, 2005). To test whether decreasing cellular PA might also change actin filament levels, we applied 1-butanol to poppy pollen at concentrations between 10 and 100 mM for 30 min. Filamentous levels were quantified in the fluorimeter with the assay described above. Relative levels of filamentous actin follow-
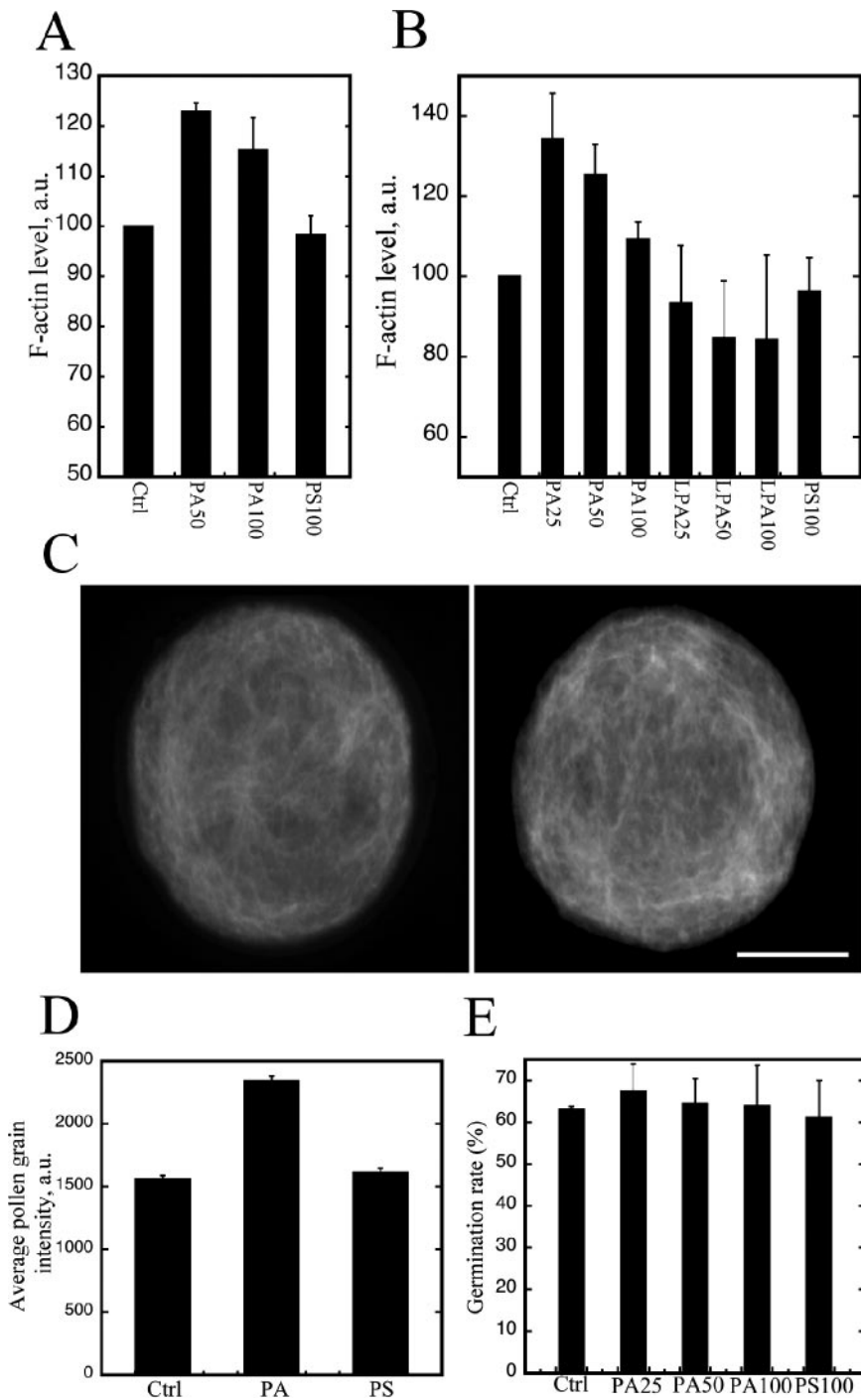
**Figure 2.** PA treatment elevates the level of filamentous actin. (A) Filamentous actin was quantified by fixing *Arabidopsis* suspension cells and incubating them with a saturating concentration of Alexa 488-phalloidin. After washes to remove unbound phalloidin, Alexa-phalloidin was stripped from the actin filaments by methanol treatment and quantified in the fluorometer. To normalize for cell numbers, ethidium bromide was included in the original staining mixture, and fluorescence was expressed as a ratio of phalloidin divided by ethidium values. Ctrl (no treatment), PA50 (50 $\mu$M PA), PA100 (100 $\mu$M PA), and PS100 (100 $\mu$M PS) treatments were performed for 2 h by addition of phospholipid to the culture medium. Each bar represents the mean value ($\pm$SD) from three separate experiments. The ratio of phalloidin/ ethidium bromide for the control population was given a value of 100% for each experiment. (B) Filamentous actin was quantified by fixing *Papaver rhoeas* pollen and incubating with a saturating concentration of Alexa 488-phalloidin. Bound fluorescent-phalloidin was removed from pollen with methanol and quantified by fluorimetry. Ctrl (no treatment), PA25 (25 $\mu$M PA), PA50 (50 $\mu$M PA), PA100 (100 $\mu$M PA), and PS100 (100 $\mu$M PS). Additional treatments included LPA at 25, 50, and 100 $\mu$M. Each bar represents the mean value ($\pm$SD) from three separate experiments. The control fluorescence was set to 100% for each experiment. (C) The effect of exogenous PA treatment on the actin cytoskeleton of pollen grain was visualized by confocal laser scanning microscopy after staining with Alexa-488-phalloidin. Left, a pollen grain treated with 100 $\mu$M PS; right, a pollen grain treated with 25 $\mu$M PA. Confocal settings and image collection and display parameters were identical between treatments. Images shown are z-series stacks of 40 optical sections. Scale bar, 10 $\mu$m. (D) The average pixel intensity was measured for the pollen grains by wide-field fluorescence microscopy. Ctrl (no treatment), PA (25 $\mu$M PA), PS (100 $\mu$M PS). More than 100 grains were measured for each treatment and the mean values ($\pm$SD) are plotted. (E) The effect of exogenous PA on the pollen germination rate. At least 200 pollen grains were counted for each treatment. Each bar represents the mean value from three experiments. Error bars, SD.

ing 10, 50, and 100 mM 1-butanol treatment were 108 $\pm$ 12, 101 $\pm$ 10, 108 $\pm$ 6%, respectively. Moreover, treatments for 1 h with 100 mM 1-butanol also did not significantly reduce actin filament levels (102 $\pm$ 5%). The inactive secondary alcohol, sec-butanol, at 100 mM also had little effect on actin filament levels (106 $\pm$ 2%). Thus, increasing cellular PA stimulates actin polymerization, whereas reducing PA has no effect on actin filament levels.

### Arabidopsis CP Binds to Specific Acidic Phospholipids

Many eukaryotic ABPs, including plant profilin, ADF/cofilin, and capping protein (Drøbak et al., 1994; Gungabissoon et al., 1998; Huang et al., 2003), bind to PPI lipids, and this interaction regulates their association with actin (Yin and Janmey, 2003). By binding to the rapidly growing end of actin filaments, the heterodimeric CP from *Arabidopsis* (AtCP) likely plays a central role in modulating polymer levels and dynamics (Huang *et al.,* 2003). We tested the ability of AtCP to bind a variety of acidic phospholipids with protein–lipid blot overlay assays, as shown in Figure 3A. AtCP showed a marked preference for PA, but did not bind at all to other phospholipids like phosphatidylcholine, PS, or phosphatidylethanolamine. There was also reproducible (n = 3) interaction with a subset of the PPIs, including
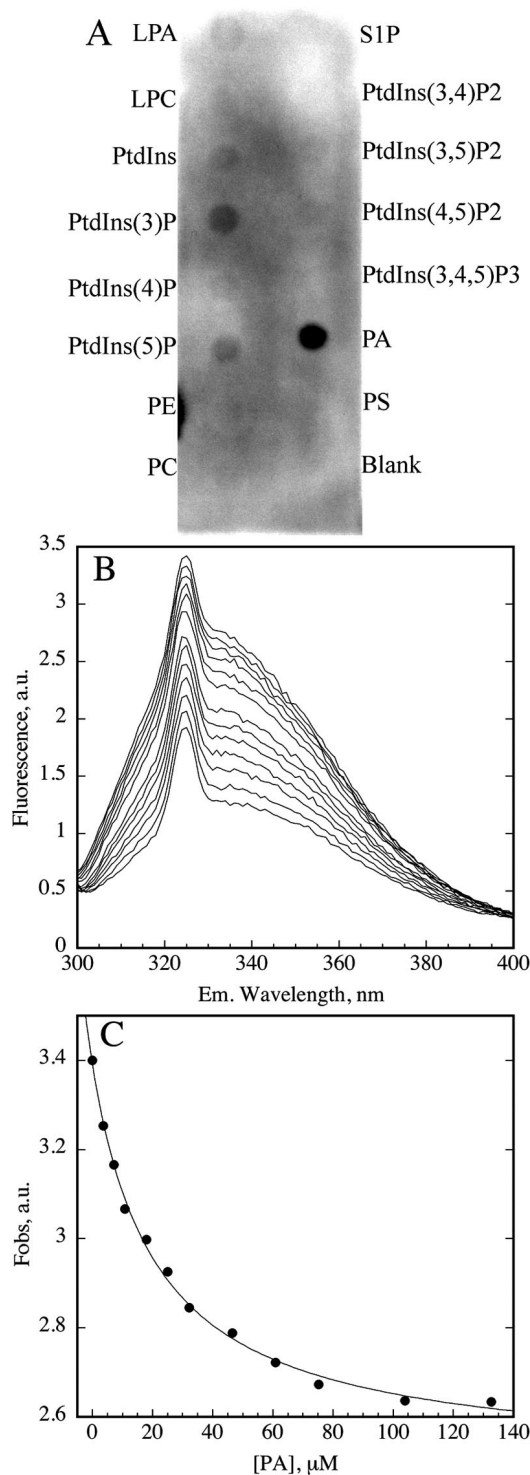
**Figure 3.** *Arabidopsis* capping protein (AtCP) binds to PA. (A) Blot overlay assays were used to detect protein–lipid interactions. PIP strips contain an array of acidic phospholipids, including lysophosphatidic acid (LPA); lysophosphocholine (LPC); phosphatidylinositol (PtdIns); PtdIns(3)P; PtdIns(4)P; PtdIns(5)P; phosphatidylethanolamine (PE); phosphatidylcholine (PC); sphingosine-1-phosphate (S1P); PtdIns(3,4)P$_2$; PtdIns(3,5)P$_2$; PtdIns(4,5)P$_2$; PtdIns(3,4,5)P$_3$; phosphatidic acid (PA); and phosphatidlyserine (PS). Each spot contains 100 pmol of phospholipid, and the membrane was challenged with 5 $\mu$g/ml protein (83 nM). AtCP was detected with a mixture of two polyclonal antisera raised against the $\alpha$ and $\beta$ subunits (Huang *et al.,* 2003). AtCP shows a preference for PA. (B) Tryptophan fluorescence emission spectra for AtCP. The excitation wave-

PtdIns(3)P and PtdIns(5)P, although this was noticeably weaker than for PA. Surprisingly, given the recent demonstration of AtCP regulation by PtdIns(4,5)P$_2$ (Huang *et al.,* 2003), this lipid was poorly detected on the protein–lipid overlays. Perhaps this is an artifact of the solid-phase interaction between lipids and the nitrocellulose that is used as a support for the assay.

To confirm and extend the specificity of AtCP binding to various phospholipids and to measure the affinity, assays that monitored the quenching of protein intrinsic tryptophan fluorescence upon binding PA, PtdIns(4,5)P$_2$ and LPA were performed. This method has been used routinely to study the binding of several ABPs, such as profilin (Lu *et al.,* 1996), CapG (Lin *et al.,* 1997), and villin (Kumar *et al.,* 2004) to PtdIns(4,5)P$_2$ and D3-PPIs. AtCP had an emission maximum of around 325 nm, whereas lipid vesicles alone had no fluorescence at the excitation wavelength used here. A plot of the AtCP fluorescence emission spectrum showed that with each addition of PA, the endogenous tryptophan fluorescence was reduced (Figure 3B). By fitting the data points for fluorescence emission at 325 nm to Equation 1 (*Materials and Methods*), a $K_d$ value of 21 $\mu$M was calculated (Figure 3C).

From at least three such experiments with AtCP, a mean $K_d$ value of 17 $\mu$M for PA binding, 11.4 $\mu$M for PtdIns(4,5)P$_2$ binding, and 38 $\mu$M for LPA binding were obtained (Table 1). For comparison, the affinity of mouse capping protein (MmCP) for phospholipids was also determined; mean $K_d$ values of 59 $\mu$M for PA, 7.8 $\mu$M for PtdIns(4,5)P$_2$, and 36 $\mu$M for LPA were measured (Table 1). Similar experiments with PtdIns and both capping proteins showed no appreciable shift in endogenous fluorescence and therefore were not modeled. Moreover, no apparent binding between AtCP and PtdIns(3,4)P$_2$, PtdIns(3,5)P$_2$, PtdIns(3)P, PtdIns(4)P, PtdIns(5)P, PS, or DAG was detected (unpublished data). Thus, MmCP has a preference of PtdIns(4,5)P$_2$ > {LPA and PA} ≫ PtdIns, whereas AtCP prefers PtdIns(4,5)P$_2$ and PA. The stoichiometry of binding ($\rho$) ranged from 1.6 to 2.7 lipid molecules per molecule of CP (Table 1). Generally, the stoichiometry of PA binding was higher than that observed for PtdIns(4,5)P$_2$. By comparing with published values for binding of PtdIns(4,5)P$_2$ to CapG ($K_d$ = 6–24 $\mu$M), villin ($K_d$ = 39 $\mu$M), and profilin ($K_d$ = 20–35 $\mu$M; Lu *et al.,* 1996; Lin *et al.,* 1997), we can conclude that AtCP also binds to PA and PtdIns(4,5)P$_2$ with moderate affinity. The results from these solution-based interactions of AtCP and phospholipid micelles differed from the blot overlays, in that binding to PtdIns(4,5)P$_2$ was not indicated by the latter. However, the interaction with both PA and PtdIns(4,5)P$_2$ are confirmed by analysis of the effects on actin-binding activity.

### PA Regulates AtCP Function

To test whether PA binding regulates the actin-based function of AtCP, several kinetic and steady state assays of actin polymerization and depolymerization were performed.

length is 292 nm and emission curves for 0.1 $\mu$M AtCP are shown. The top curve is AtCP alone and the remaining curves are for a titration with PA ranging from 3.6 to 132 $\mu$M. Addition of PA causes a reduction or quenching of intrinsic fluorescence. (C) The observed fluorescence ($F_{obs}$) at 325 nm as a function of [PA] was plotted for the experiment in B. The data were fit to Equation 1 (*Materials and Methods*) to derive a $K_d$ value. For this representative experiment, the predicted $K_d$ was 21 $\mu$M. a.u., arbitrary fluorescence units.

**Table 1.** Mean $K_d$ values for experiments with AtCP and MmCP

| | PA | | LPA | | PtdIns(4,5)P$_2$ | | PtdIns | |
|---|---|---|---|---|---|---|---|---|
| | $K_d$ | $\rho^a$ | $K_d$ | $\rho$ | $K_d$ | $\rho$ | $K_d$ | $\rho$ |
| AtCP | $17 \pm 2$ | 2.4 | $38 \pm 13$ | 2.7 | $11.4 \pm 1.3$ | 1.6 | No value[b] | ND |
| MmCP | $59 \pm 6$ | 2.5 | $36 \pm 11$ | 1.7 | $7.8 \pm 0.6$ | 1.7 | No value[b] | ND |

Values are mean $\pm$ SD (n $\geq$ 3) expressed in $\mu$M for binding to phospholipids from experiments of intrinsic tryptophan fluorescence titration.
[a] $\rho$ is the stoichiometry of lipid molecule:protein interaction as calculated according to Stinson and Holbrook (1973).
[b] Experiments were performed, but no detectable changes in fluorescence emission were detected. This is consistent with no interaction or an extremely low-affinity interaction between protein and lipid micelles.

### PA Inhibits the Ability of AtCP to Nucleate Actin Filament Assembly

*Arabidopsis* CP enhances the nucleation of filaments during assembly from monomeric actin (Huang *et al.*, 2003). The effect of PA on AtCP-induced actin assembly was examined. The results showed that the initial lag corresponding to the nucleation step decreased in the presence of 500 nM AtCP (Figure 4A). This effect was inhibited in a dose-dependent manner by the presence of PA (Figure 4A). Similar results were obtained for PtdIns(4,5)P$_2$ (Figure 4B), but compared with PA at the same concentrations, the efficiency of inhibition appeared somewhat lower. For example, 150 $\mu$M PtdIns(4,5)P$_2$ (Figure 4B) is required to give about the same effect as 100 $\mu$M PA (Figure 4A). PtdIns had almost no effect on nucleation activity at the highest concentration tested (Figure 4B), consistent with the tryptophan fluorescence data that demonstrated no significant binding to AtCP. Polymerization of 2 $\mu$M actin in the presence of 150 $\mu$M PA or PtdIns(4,5)P$_2$ (Figure 4, A and B) showed no difference from the curves obtained with actin alone (unpublished data), confirming that the presence of lipid does not alter actin assembly directly.

### PA Inhibits the Filament-capping Activity of AtCP

*Arabidopsis* CP binds with high-affinity ($K_d$ 12–24 nM) to the barbed ends of actin filaments and prevents dilution-mediated filament depolymerization (Huang *et al.*, 2003). In the present experiments, depolymerization of 5 $\mu$M filamentous actin by a 25-fold dilution with buffer was prevented in the presence of 500 nM AtCP. This is due to AtCP binding the barbed ends of actin filaments and preventing subunit loss. PA inhibited this activity in a dose-dependent manner (Figure 5A). PtdIns(4,5)P$_2$ gave similar results, but was somewhat less efficient than PA at the same concentrations (Figure 4B). By contrast, 150 $\mu$M PtdIns had a minimal effect (Figure 5B). Addition of 200 $\mu$M PA (Figure 5A) or 150 $\mu$M PtdIns(4,5)P$_2$ (Figure 5B) in the absence of AtCP showed no difference from actin alone (unpublished data), indicating that phospholipids do not prevent filament depolymerization directly.

To compare the effect of different phospholipids on capping activity, we performed experiments similar to those described above and plotted the initial depolymerization rate as a function of [phospholipid]. As shown in Figure 5C, 300 $\mu$M PA did not further increase the initial depolymerization rate, and the concentration of PA required to increase initial depolymerization rate to half maximum was ~100 $\mu$M. The activity of PtdIns(4,5)P$_2$ was quite similar to PA, and LPA also inhibited capping of barbed ends but was less efficient than PA. However, PtdIns had little effect on capping activity. The result of these comparisons is roughly consistent with results from fluorescence microscopy as described below.

### Single Actin Filament Imaging Confirms the Inhibition of Capping Activity

Fluorescence microscopy has been used to show that a population of actin filaments is significantly shorter than controls when polymerized in the presence of AtCP (Huang *et al.*, 2003). This is consistent with AtCP blocking assembly from barbed
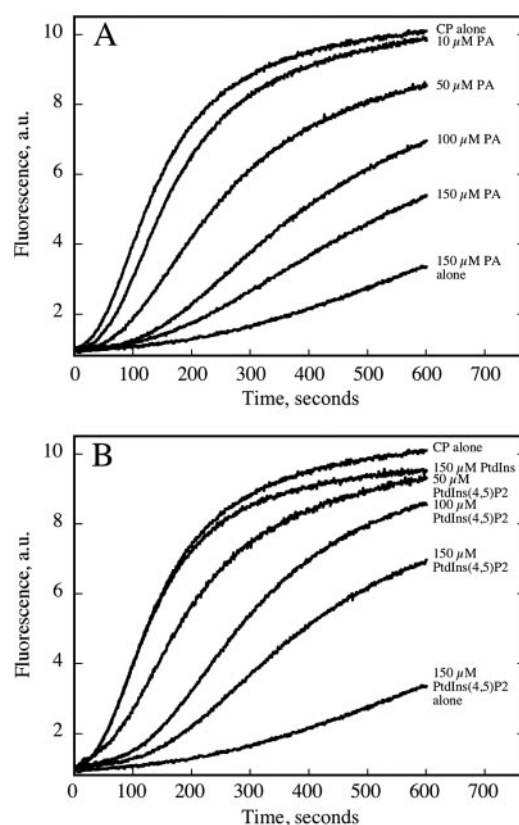


**Figure 4.** PA inhibits the actin nucleation activity of AtCP. PA and PtdIns(4,5)P$_2$ at varying concentrations were incubated for 5 min with 500 nM AtCP before incubation with 2 $\mu$M actin (5% pyrene-labeled). Pyrene fluorescence is plotted versus time after addition of KMEI buffer to initiate polymerization. (A) The effect of PA on AtCP-induced actin nucleation. From top to bottom, the curves are 500 nM AtCP alone, 500 nM AtCP + 10 $\mu$M PA, 500 nM AtCP + 50 $\mu$M PA, 500 nM AtCP + 100 $\mu$M PA, 500 nM AtCP + 150 $\mu$M PA, and 150 $\mu$M PA alone. (B) The effect of PtdIns(4,5)P$_2$ and PtdIns on AtCP-induced actin nucleation. From top to bottom: 500 nM AtCP alone, 500 nM AtCP + 150 $\mu$M PtdIns, 500 nM AtCP + 50 $\mu$M PtdIns(4,5)P$_2$, 500 nM AtCP + 100 $\mu$M PtdIns(4,5)P$_2$, 500 nM AtCP + 150 $\mu$M PtdIns(4,5)P$_2$, and 150 $\mu$M PtdIns(4,5)P$_2$ alone.
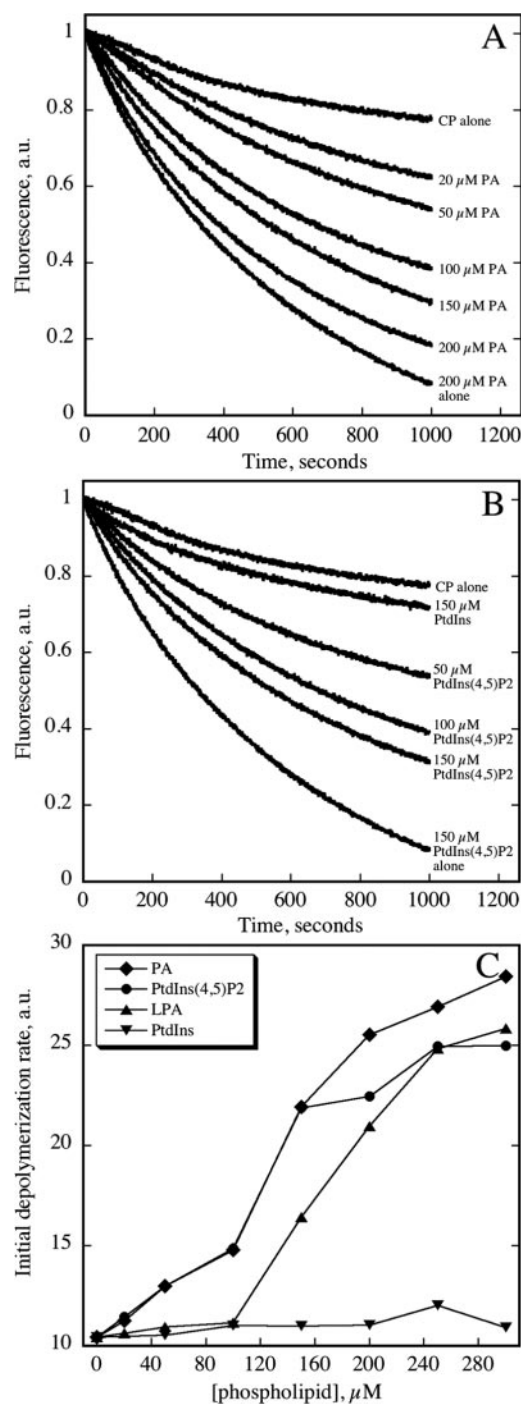
**Figure 5.** Barbed-end capping activity is inhibited by PA. PA inhibits the capping activity of AtCP as determined by a dilution-mediated depolymerization assay. AtCP, 500 nM, was preincubated with varying concentrations of phospholipids for 5 min before incubation with 5 $\mu$M filamentous actin for 5 min. Then, the mixture was diluted 25-fold with buffer. (A) The effect of PA on actin depolymerization, from top to bottom: 500 nM AtCP alone, 500 nM AtCP + 20 $\mu$M PA, 500 nM AtCP + 50 $\mu$M PA, 500 nM AtCP + 100 $\mu$M PA, 500 nM AtCP + 150 $\mu$M PA, 500 nM AtCP + 200 $\mu$M PA, and 200 $\mu$M PA alone. (B) The effect of PtdIns(4,5)P$_2$ and PtdIns on actin depolymerization, from top to bottom: 500 nM AtCP alone, 500 nM AtCP + 150 $\mu$M PtdIns, 500 nM AtCP + 50 $\mu$M PtdIns(4,5)P$_2$, 500 nM AtCP + 100 $\mu$M PtdIns(4,5)P$_2$, 500 nM AtCP + 150 $\mu$M PtdIns(4,5)P$_2$, and 150 $\mu$M PtdIns(4,5)P$_2$ alone. (C) The initial depolymerization rate from 0 to 150 s was plotted as a function of [phospholipid] from experiments like those in A and B.

ends, inhibiting filament annealing, as well as increasing the number of actin filaments during assembly by nucleation. When 4 $\mu$M actin was assembled in the presence of 500 nM AtCP, the mean length of filaments (0.6 ± 0.6 $\mu$m) was reduced substantially and the length distribution was quite uniform (Figure 6A). However, when PA was added to 20 $\mu$M (Figure 6B), 50 $\mu$M (Figure 6C), 100 $\mu$M (Figure 6D), 150 $\mu$M (Figure 6E), 200 $\mu$M (Figure 6F), and 250 $\mu$M (Figure 6G), the mean length of filaments was 1.0 ± 0.9, 1.4 ± 1.2, 3 ± 2, 4 ± 3, 5 ± 3, and 6 ± 4 $\mu$m, respectively. For comparison, 250 $\mu$M PtdIns had little effect (mean length of 0.8 ± 0.7 $\mu$m, Figure 6H). At the highest concentration of PA tested, the length of actin filaments was virtually identical to that for actin in the absence of AtCP (mean length of 6 ± 4 $\mu$m). Moreover, the mean length of actin filaments in the presence of 250 $\mu$M PA (but without AtCP) was almost the same as that of actin alone, suggesting that PA does not affect actin polymerization directly but rather acts through capping protein. These results demonstrated that PA prevents AtCP from binding the barbed ends of actin filaments, or nucleating filament formation, in a dose-dependent manner.

To compare the effect of different phospholipids on AtCP activity, the fluorescence microscopy assay was repeated with PtdIns(4,5)P$_2$ LPA and PtdIns and filament lengths measured (Figure 7). The effect of PA on filament length saturated at ~250 $\mu$M or 500:1 lipid:AtCP. The half maximal effect of lipid micelles was observed at ~120 $\mu$M PA. By comparison, PtdIns(4,5)P$_2$ and LPA also prevented the capping of actin filaments but were less efficient than PA, and PtdIns had no effect on capping activity.

### Uncapping of Filament Ends Is Induced by PA

The previous assays demonstrated that AtCP binding to filament ends is prevented in the presence of specific phospholipids. To show that PA can remove AtCP from the ends of actin filaments, seeded polymerization reactions were performed (Figure 8). In this assay, actin elongation was initiated by the addition of 1 $\mu$M actin monomer, saturated with 4 $\mu$M profilin, to 0.8 $\mu$M actin filament seeds. Profilin prevents spontaneous nucleation and/or growth from actin filament pointed ends under these conditions (Pollard and Cooper, 1984). To test whether PA will promote the dissociation of AtCP from barbed ends of actin filaments, preformed actin filament seeds were incubated with 200 nM AtCP, and then profilin-actin was added along with various concentrations of PA to initiate elongation at the barbed ends. The results showed that AtCP inhibited the elongation at barbed ends almost completely in the absence of lipid. Increasing amounts of PA correlate with an enhancement of the initial polymerization rate, which is interpreted as the uncapping of filament barbed ends and assembly of the profilin–actin complex onto preexisting filaments (Figure 8A). In the presence of PA, lower plateau levels for actin polymerization are reached, presumably because AtCP reaches an equilibrium between free protein and protein bound to lipid or filament ends. In the absence of AtCP the elongation with 1 $\mu$M actin monomer in the presence of 200 $\mu$M PA (Figure 8A, top curve) showed no difference when compared with actin alone (unpublished data), confirming that PA does not stimulate profilin–actin assembly directly.

Uncapping in the above experiments could result from PA binding to AtCP on the barbed end of a filament and cause a decrease in the affinity for filament ends. Alternatively, AtCP may have a high endogenous rate of dissociation from filaments and PA binding to free CP prevents reassociation with a filament. To distinguish these possible mechanisms, we determined association and dissociation rate constants
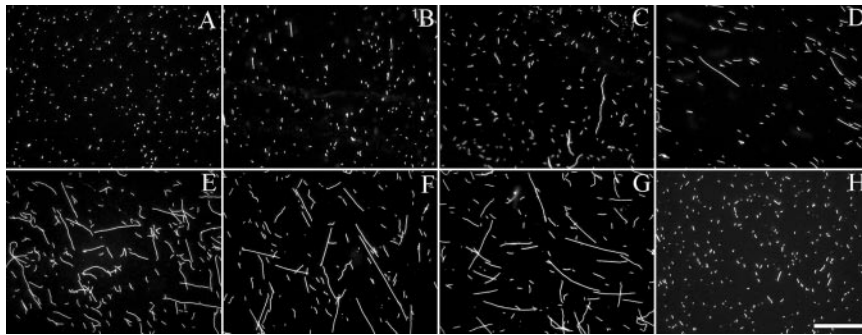
**Figure 6.** PA allows extensive actin filament growth in the presence of AtCP. Fluorescence micrographs of individual actin filaments assembled from 4 $\mu$M Mg-ATP-actin monomer in the presence of AtCP are shown. To test the effect of PA and PtdIns on AtCP activity, AtCP was preincubated with varying amounts of lipid micelles for 5 min. Scale bar, 10 $\mu$m. (A) 500 nM AtCP alone; (B) 500 nM AtCP + 20 $\mu$M PA; (C) 500 nM AtCP + 50 $\mu$M PA; (D) 500 nM AtCP + 100 $\mu$M PA; (E) 500 nM AtCP + 150 $\mu$M PA; (F) 500 nM AtCP + 200 $\mu$M PA; (G) 500 nM AtCP + 250 $\mu$M PA; and (H) 500 nM AtCP + 250 $\mu$M PtdIns.

for AtCP binding to the barbed end of actin filaments using kinetic simulations and a model for actin elongation in the presence of capping proteins. Actin monomers bound to profilin were polymerized by elongation of actin filament seeds in the presence of varying concentration of AtCP. For uncapped filaments, we used the barbed end association rate constant $k_+ = 10$ $\mu$M$^{-1}$ s$^{-1}$ and dissociation rate constant $k_- = 1.4$ s$^{-1}$. The concentration of actin filament ends (N) was calculated from the initial rate of elongation in the absence of capping protein (Huang *et al.*, 2003). We searched for the capping rate constant for AtCP binding to the barbed ends of actin filaments according to the simulation that best fit three independent kinetics experiments. The dissociation rate constant of AtCP from barbed ends, $k_- = 0.0003 \pm 0.0001$ s$^{-1}$ is similar to the off-rate constant for muscle CP ($4 \times 10^{-4}$ s$^{-1}$; Schafer *et al.*, 1996). However, the association rate constant $k_+ = 0.07 \pm 0.05$ $\mu$M$^{-1}$ s$^{-1}$ was slower than the association rate constant for muscle CP (3.5 $\mu$M$^{-1}$ s$^{-1}$; Schafer *et al.*, 1996) consistent with the lower affinity of *Arabidopsis* capping protein for the barbed ends of vertebrate actin filaments. These results demonstrate that dissociation of AtCP from filament ends in the absence of phospholipids is rather slow, and that PA binding to CP likely uncaps filaments by changing the affinity of CP for barbed ends.
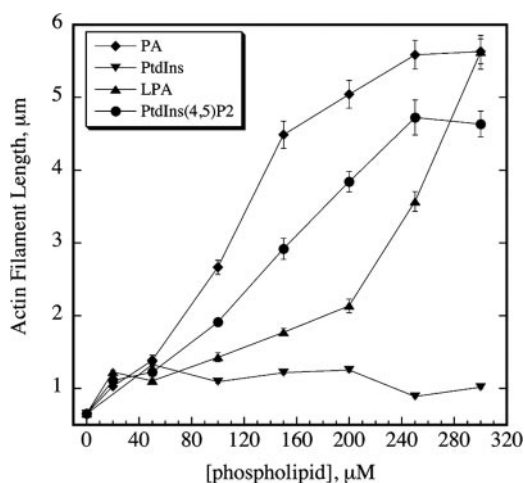


**Figure 7.** Comparison of the effects of different phospholipids on capping activity. Fluorescence light microscope experiments, like those shown in Figure 6, were performed in the presence of 500 nM AtCP and varying concentrations of PA, LPA, PtdIns(4,5)P$_2$, and PtdIns. Mean filament length ($\pm$SEM) from several micrographs of each treatment was plotted versus phospholipid concentration.

## DISCUSSION

In this study, we show that the heterodimeric actin filament capping protein from *A. thaliana* (AtCP) binds with moderate affinity to PA and that its activity is regulated by the interaction with phospholipids. Specifically, binding to PA inhibits the ability of AtCP to bind the barbed ends of actin filaments and to nucleate filament assembly. In the presence of PA, CP does not reduce the lag period for assembly from actin monomers and it fails to block dilution-mediated depolymerization of actin filaments. PA can also induce the uncapping of filament barbed ends during seeded polymerization reactions, thereby facilitating assembly of actin filaments from a pool of profilin–actin. By quantitative analysis of changes in endogenous tryptophan fluorescence, a binding constant ($K_d$) of 17 $\mu$M and approximate stoichiometry of 1:2.4 mole of protein to mole of PA were determined. These values are similar to the apparent binding of PtdIns(4,5)P$_2$ ($K_d = 11$ $\mu$M and stoichiometry of 1:1.6), which we had shown previously regulates the filament capping activity of AtCP (Huang *et al.*, 2003). To our knowledge, this is the first evidence that any plant actin-binding protein binds to and is regulated by the abundant phospholipid, PA. The consequence of this interaction is that when cellular PA levels increase, for example, during wounding, filament ends become uncapped and net actin polymerization can occur. Indeed, we confirm earlier results that exogenous PA treatments stimulate actin polymerization in suspension cells and pollen tubes.

The specificity of lipid micelle interaction with AtCP is as follows: {PtdIns(4,5)P$_2$ and PA} > LPA ≫ PtdIns. This is somewhat different from what is found by the blot overlay assay, where binding to PtdIns(4,5)P$_2$ and LPA was just as weak as or worse than binding to PtdIns. To confirm the ability of the solution-based micelle binding assay to detect specific changes, we measured the binding of recombinant mouse CP (MmCP) to different phospholipids. Here, we found that MmCP shows the preference: PtdIns(4,5)P$_2$ > {LPA and PA} ≫ PtdIns. This is consistent with the results of Cooper and colleagues for chicken CapZ showing that PtdIns(4,5)P$_2$ and PtdIns(4)P are capable of blocking barbed-end capping activity, whereas PA, PtdIns, and PtdIns(3,4,5)P$_3$ have little or no effect on activity (Heiss and Cooper, 1991; Schafer *et al.*, 1996). Therefore, the ability of CP to bind PA may be limited to the plant kingdom. We also confirmed the ability of different phospholipids to interact with CP indirectly by measuring the ability of selected lipids to alter actin-binding properties. Fluorimetry and light microscope assays corroborate the finding that PA and PtdIns(4,5)P$_2$ have roughly similar affinities for AtCP. Although the affinity of AtCP for PtdIns(4,5)P$_2$ may be slightly higher, the interaction with PA is perhaps more relevant

**Figure 8.** PA promotes the dissociation of AtCP from the barbed ends of actin filaments. (A) Except for the top curve, preformed actin filament seeds (0.8 $\mu$M) were incubated with 200 nM AtCP for 5 min at room temperature. Elongation of filaments from the barbed ends of the seeds was initiated by addition of 1 $\mu$M actin monomer saturated with 4 $\mu$M human profilin I. Polymerization reactions were performed with varying concentrations of PA, ranging from 0 to 200 $\mu$M, and these are listed at right of each polymerization curve. The change in pyrene-actin fluorescence accompanying polymerization was plotted versus time after addition of actin monomer. In the absence of capping protein, PA does not enhance assembly of profilin–actin (top curve) relative to elongation in the absence of lipid (unpublished data). (B) Kinetic simulation of data from the elongation assay was used to determine dissociation and association rate constants for AtCP-binding filament barbed ends. Elongation of filaments from the barbed ends of the seeds (1.2 $\mu$M) was initiated by addition of seeds to a solution containing 1 $\mu$M actin monomer saturated with 4 $\mu$M human profilin I. Elongation experiments were performed with varying concentrations of AtCP (0, 100, 200, 300, and 500 nM; curves from top to bottom) added to the profilin-bound actin monomers before addition to the actin filaments seeds. The noisy dotted line is the actual time course for polymerization from actin filaments seeds. Solid lines are the simulation for each reaction according to the model for actin elongation in presence of capping protein using FITSIM (see *Materials and Methods*). Association and dissociation rate constants for AtCP binding to actin filaments barbed ends were respectively, $k_+ = 0.035\ \mu M^{-1}\ s^{-1}$ and $k_- = 0.0002\ s^{-1}$ for this representative experiment.
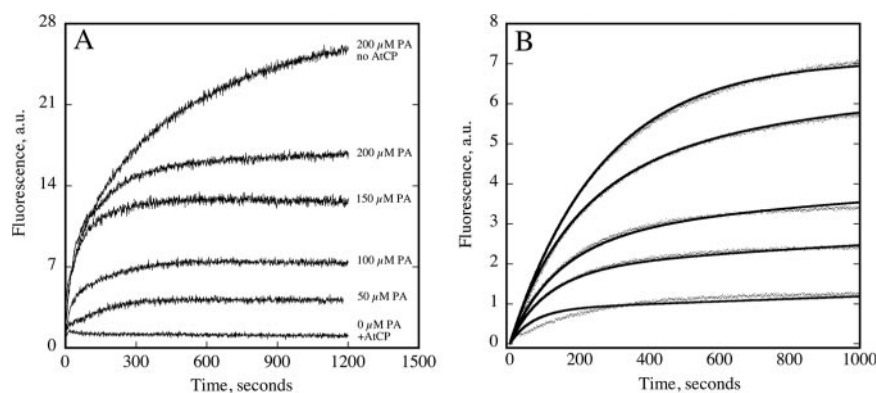
within the cell as this phospholipid species is substantially more abundant in plant cells than is PtdIns(4,5)P$_2$. Estimates of PA concentration in *Arabidopsis* leaves range from 50 to 100 $\mu$M, and these levels may increase by more than 50% in response to stress or phytohormone application (Li *et al.,* 2004; Zhang *et al.,* 2004), whereas PtdIns(4,5)P$_2$ levels are likely to be 10- to 100-fold lower (Drøbak, 1993). In pollen tubes, the endogenous levels of PA are nearly a 100 times higher than are PtdIns(4,5)P$_2$ levels and PA can increase up to sevenfold following hypo-osmotic stress (Zonia and Munnik, 2004).

The interaction of PPIs with CP from vertebrates, lower eukaryotes, and plants is now well established (Haus *et al.,* 1991; Heiss and Cooper, 1991; Amatruda and Cooper, 1992; Schafer *et al.,* 1996; Sizonenko *et al.,* 1996; Huang *et al.,* 2003). Although the binding site(s) on the surface of CP remains to be determined (Wear and Cooper, 2004b), there is some evidence from gel filration analysis that the $\alpha$-subunit of muscle CP binds to PtdIns(4,5)P$_2$ (Heiss and Cooper, 1991). Recently, Yamashita *et al.* (2003) solved the x-ray crystal structure for chicken CapZ. Their study reveals that the $\alpha1/\beta1$ heterodimer forms a compact structure resembling a mushroom with pseudotwofold rotational symmetry. The two C-terminal regions, of approximately 30 residues each, lie on the "cap" of the mushroom and each contains a short stretch of amphipathic $\alpha$-helix. These are predicted to form flexible "tentacles" that make intimate contact with the barbed end of an actin filament. Biochemical, molecular, and genetic data support this model and give evidence for a slightly greater importance of the C-terminus of the $\alpha$-subunit (Kim *et al.,* 2004; Wear *et al.,* 2003). However, recent data indicate that the $\alpha$-subunit C-terminus may be immobilized on the surface of CP and the hydrophobic residues of the amphipathic helix masked by interaction with the underlying $\beta$-sheet (Wear and Cooper, 2004a). Although a number of PA-binding sequences are now known from different proteins, they share rather little primary sequence similarity, other than a few conserved basic amino acids, making sequence-based predictions rather difficult (Testerink and Munnik, 2005). There is reasonable similarity (45% over 33 amino acids), however, between the C-terminal region from the AtCP $\alpha$-subunit and a recently identified PA-binding

sequence from the *Arabidopsis* protein phosphatase 2C, ABI1 (Zhang *et al.,* 2004; Figure 9). Indeed, several basic amino acids are absolutely conserved, including one arginine (R73) that was demonstrated to be necessary for PA binding by ABI1 (Figure 9). The C-terminal region of chicken CP$\alpha$1 shares less overall similarity (30%) with the same region from ABI1 (Figure 9), perhaps explaining why vertebrate CP bound rather poorly to PA in our studies. We predict, therefore, that the C-terminus of AtCPA constitutes a PA-binding motif. Interaction between CP and phospholipids on a membrane surface would then sterically hinder the binding to an actin filament and thereby prevent capping. An alternative model, proposed by Yamashita *et al.* (2003) based on the location of two bound nitrate ion sites on the overall fold of chicken CapZ, is that the polar head group of a PPI makes contact with a region of the $\beta$ subunit immediately adjacent to the C-terminal region of the $\alpha$-subunit. Both models require additional structural, molecular or biochemical analyses to test their validity.

Evidence for a connection between PLD signaling, or PA production, and the cytoskeleton is emerging rapidly, especially in plant systems (Meijer and Munnik, 2003; Wang, 2004; Testerink and Munnik, 2005). PLD isoforms from plants, animals, and bacteria are quite clearly regulated by interactions with the actin cytoskeleton (Lee *et al.,* 2001; Kusner *et al.,* 2002, 2003). Like human PLD1, the activity of a recombinant PLD$\beta$ isoform from *Arabidopsis* is modulated in a polymerization state–dependent manner by actin; monomeric actin inhibits PLD activity, whereas filamentous actin stimulates it (Kusner *et al.,* 2003). PLD$\beta$ can also be cosedimented with actin filaments in vitro. These studies all suggest an intimate relationship between membrane targeting of PLD and regulation of its activity by the cortical cytoskeleton.

Pollen tubes extend by a tip-growth mechanism that requires precisely orchestrated changes in actin cytoskeletal dynamics, cytoplasmic ion fluxes, vesicle trafficking events, and phospholipid turnover. Constitutive PLD activity in pollen tubes produces large amounts of PA that turn over rapidly, and the level of PA can increase or decrease substantially in response to osmotic stress (Dorne *et al.,* 1988; Zonia and Munnik, 2004). Hindering the PLD activity and

```
ABI1        66 S R K V L I S R I N S P N L N M K E S A A A D I V V V D I S A G D 98
AtCPA      275 R R K L P V T R T L P W Q N T L Q F S L T R E V E K E L G L G K 308
OsCPA      265 R R R L P V T R S K I N W G S - - - A I G S Y R L G K N A A E G K 297
Chicken A1 259 R R Q L P V T R T K I D W N - - - - K I L S Y K I G K E M Q N A 286
S.cerevisiae 239 R R R L P V T R S K I N W G S - - - A I G S Y R L G K N A A E G K 268
```

**Figure 9.** The C-terminal 'tentacle' domain from AtCPA may be a phospholipid-binding site. Shown are sequence alignments between the minimal sequence from ABI1 which is sufficient for binding to PA (Zhang *et al.,* 2004), less 6 amino acids, and the C-terminal domain of capping proteins. Crystallographic structure, molecular and biochemical data suggest that this domain forms a flexible "tentacle" involved in actin binding. The gene accession numbers of proteins used for the alignment are as follows: ABI1 (NM_118741); *Arabidopsis thaliana* α subunit (AtCPA; NM_111425); *Oryza sativa* α subunit (OsCPA; AP005247.2); chicken α1 subunit (M25534); and *S. cerevisiae* α subunit (X61398). Alignments were prepared with the ClustalW algorithm in MacVector v.7.1.1 software (Accelrys, Madison, WI). Gaps were introduced to optimize the alignment and residues that are conserved in >50% of the sequences are highlighted.

reducing the production of PA with 1-butanol treatments results in the inhibition of pollen germination, cessation of pollen tube growth, and reversible loss of cell polarity, demonstrating that PA is essential for normal tip growth (Potocký *et al.,* 2003; Monteiro *et al.,* 2005a). The turnover of PA may be linked to the regulation of other phospholipids, to intracellular membrane trafficking, or to the control of the tip-focused, oscillatory cytosolic calcium gradient (Potocký *et al.,* 2003; Monteiro *et al.,* 2005a,b). There may also be direct or indirect links to cytoskeletal organization and function; decreased PA causes an increase in bundled actin filaments in pollen tubes (Monteiro *et al.,* 2005a), excess PA results in an increase in tip actin filaments (Monteiro *et al.,* 2005b), and the microtubule-stabilizing agent taxol can overcome the inhibitory effects of 1-butanol (Potocký *et al.,* 2003). In our study, we did not observe any changes in actin filament levels due to 1-butanol treatment, but did find that elevated cellular PA could quantitatively increase actin filament levels. The identification of CP as stimulus-response modulator provides a mechanism to link cytoskeletal dynamics directly to PA turnover in pollen.

Lee *et al.* (2003) were the first to show that actin filament levels in plant suspension-cultured cells increased after PA treatment and they propose a pathway whereby PA indirectly leads to increases in filamentous actin via activation of a protein kinase. In this article, we report that short treatments with low levels of exogenous PA result in up to a 40% increase in actin filament levels in pollen and *Arabidopsis* suspension cells. At a biochemical level, we show that PA binds directly to CP and prevents binding or uncaps filament barbed ends. This provides a potential direct link between changes in PA levels and actin cytoskeleton remodeling in the plant cell. We propose a mechanism for actin cytoskeleton response to elevated levels of PA. Our simple model is that PA dissociates CP from the actin filament barbed end, allowing profilin–actin complex to add onto the free barbed ends and promotes filament elongation. As shown in Figure 10, in the unstimulated cell (left), only a small portion of total actin is in the filamentous form. This is consistent with measurements from pollen and suspension cultured cells (Gibbon *et al.,* 1999; Snowman *et al.,* 2002; Lee *et al.,* 2003; Wang *et al.,* 2005), where as little as 2–10% of the total actin pool is present in actin filaments. Additional measurements from pollen indicate that the actin monomer pool is buffered by a nearly equimolar amount of profilin (100–200 μM: Gibbon *et al.,* 1999; Snowman *et al.,* 2002). In the presence of capped filament ends, monomeric actin is
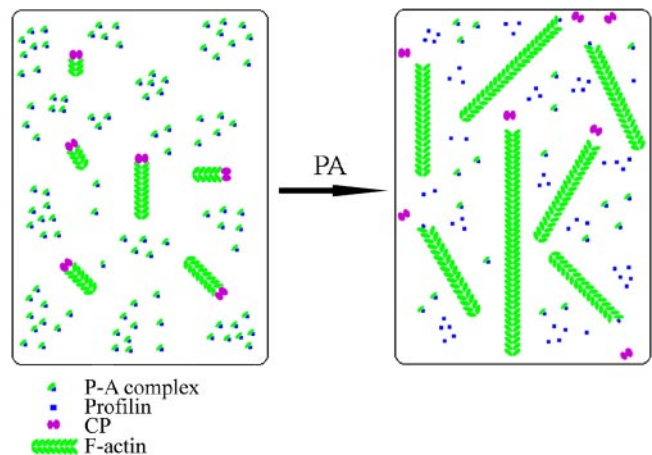


**Figure 10.** A simple model for actin cytoskeleton remodeling after PA treatment. In an unstimulated cell (left), the barbed ends of the actin filaments are mostly capped by CP. This prevents the addition of profilin–actin complex (P-A complex) onto the barbed ends, and results in a large pool of monomeric actin and relatively little filamentous actin. When PA levels increase (right), for example, during a wound or stress response, CP dissociates from the actin filament barbed end. This allows the profilin–actin complex to add onto the free barbed ends and results in a large increase in filamentous actin levels.

"sequestered" and profilin functions to suppress actin nucleation and prevents addition to filament pointed ends (Pollard and Cooper, 1984; Kang *et al.,* 1999). We proposed previously that CP acts in concert with profilin to maintain this large actin monomer pool (Huang *et al.,* 2003; Staiger and Hussey, 2004). However, after PA levels increase in a stimulated cell (Figure 10, right), CP dissociates from the barbed ends of actin filaments. The slow dissociation rate constant for AtCP from the barbed ends in absence of PA, corresponding to a half-time of dissociation of 38 min, suggests that PA binding to AtCP increases the dissociation rate constant of AtCP from the barbed ends. Consequently, profilin–actin complex can add onto the free barbed ends of the filaments and increase the level of filamentous actin. Where such events occur in the cell may also be an important consideration. The subcellular distribution of PA pools within plant cells is not known, although some native PA-binding proteins accumulate at the plasma membrane (Zhang *et al.,* 2004), and in mammalian cells, PA is abundant on the plasma membrane, ER, Golgi and endosomal membranes (Rizzo *et al.,* 2000; Baillie *et al.,* 2002; Loewen *et al.,* 2004). In our study and that of Potocký *et al.* (2003), exogenously supplied fluorescent PA showed association with an intracellular compartment or organelle but little or no plasma membrane labeling. We speculate that local uncapping of cytoplasmic actin filaments through PA binding to CP will allow actin polymerization on organelles and thereby contribute to motility events. Further tests of these global and local models for PA regulation of actin polymerization will require quantification of actin filament levels in stressed plant cells, or in mutants that elevate or depress cellular PA levels, as well as subcellular localization of CP and PA pools.

## ACKNOWLEDGMENTS

# REFERENCES

Amatruda, J. F., and Cooper, J. A. (1992). Purification, characterization, and immunofluorescence localization of *Saccharomyces cerevisiae* capping protein. J. Cell Biol. *117*, 1067–1076.

Anthony, R. G., Henriques, R., Helfer, A., Mészáros, T., Rios, G., Testerink, C., Munnik, T., Deák, M., Koncz, C., and Bögre, L. (2004). A protein kinase target of a PDK1 signaling pathway is involved in root hair growth in *Arabidopsis.* EMBO J. *23*, 572–581.

Baillie, G. S. *et al.* (2002). TAPAS-1, a novel microdomain within the unique N-terminal region of the PDE4A1 cAMP-specific phosphodiesterase that allows rapid, $Ca^{2+}$-triggered membrane association with selectivity for interaction with phosphatidic acid. J. Biol. Chem. *277*, 28298–28309.

Barshop, B. A., Wrenn, R. F., and Frieden, C. (1983). Analysis of numerical methods of computer simulation of kinetic processes: development of KINSIM—a flexible, portable system. Anal. Biochem. *72*, 248–254.

Blanchoin, L., and Pollard, T. D. (2002). Hydrolysis of ATP by polymerized actin depends on the bound divalent cation but not profilin. Biochemistry *41*, 597–602.

Cárdenas, L., Vidali, L., Domínguez, J., Pérez, H., Sánchez, F., Hepler, P. K., and Quinto, C. (1998). Rearrangement of actin microfilaments in plant root hairs responding to *Rhizobium etli* nodulation signals. Plant Physiol. *116*, 871–877.

Dorne, A.-J., Kappler, R., Kristen, U., and Heinz, E. (1988). Lipid metabolism during germination of tobacco pollen. Phytochemistry *27*, 2027–2031.

Dowler, S., Currie, R. A., Downes, C. P., and Alessi, D. R. (1999). DAPP1, a dual adaptor for phosphotyrosine and 3-phosphoinositides. Biochem. J. *342*, 7–12.

Drøbak, B. K. (1993). Plant phosphoinositides and intracellular signaling. Plant Physiol. *102*, 705–709.

Drøbak, B. K., Franklin-Tong, V. E., and Staiger, C. J. (2004). Tansley review: the role of the actin cytoskeleton in plant cell signaling. New Phytol. *163*, 13–30.

Drøbak, B. K., Watkins, P. A. C., Valenta, R., Dove, S. K., Lloyd, C. W., and Staiger, C. J. (1994). Inhibition of plant plasma membrane phosphoinositide phospholipase C by the actin-binding protein, profilin. Plant J. *6*, 389–400.

Fraley, T. S., Tran, T. C., Corgan, A. M., Nash, C. A., Hao, J., Critchley, D. R., and Greenwood, J. A. (2003). Phosphoinositide binding inhibits α-actinin bundling activity. J. Biol. Chem. *278*, 24039–24045.

Gibbon, B. C., Kovar, D. R., and Staiger, C. J. (1999). Latrunculin B has different effects on pollen germination and tube growth. Plant Cell *11*, 2349–2363.

Gibbon, B. C., Zonia, L. E., Kovar, D. R., Hussey, P. J., and Staiger, C. J. (1998). Pollen profilin function depends on interaction with proline-rich motifs. Plant Cell *10*, 981–994.

Gross, P., Julius, C., Schmelzer, E., and Hahlbrock, K. (1993). Translocation of cytoplasm and nucleus to fungal penetration sites is associated with depolymerization of microtubules and defence gene activation in infected, cultured parsley cells. EMBO J. *12*, 1735–1744.

Gungabissoon, R. A., Jiang, C.-J., Drøbak, B. K., Maciver, S. K., and Hussey, P. J. (1998). Interaction of maize actin-depolymerising factor with actin and phosphoinositides and its inhibition of plant phospholipase C. Plant J. *16*, 689–696.

Ha, K.-S., and Exton, J. H. (1993). Activation of actin polymerization by phosphatidic acid derived from phosphatidylcholine in IIC9 fibroblasts. J. Cell Biol. *123*, 1789–1796.

Ha, K.-S., Yeo, E.-J., and Exton, J. H. (1994). Lysophosphatidic acid activation of phosphatidylcholine-hydrolising phospholipase D and actin polymerization by a pertussis toxin-sensitive mechanism. Biochem. J. *303*, 55–59.

Haus, U., Hartmann, H., Trommler, P., Noegel, A. A., and Schleicher, M. (1991). F-actin capping by Cap32/34 requires heterodimeric conformation and can be inhibited with PIP2. Biochem. Biophys. Res. Comm. *181*, 833–839.

Heiss, S. G., and Cooper, J. A. (1991). Regulation of CapZ, and actin capping protein of chicken muscle, by anionic phospholipids. Biochemistry *30*, 8753–8758.

Huang, S., Blanchoin, L., Kovar, D. R., and Staiger, C. J. (2003). *Arabidopsis* capping protein (AtCP) is a heterodimer that regulates assembly at the barbed ends of actin filaments. J. Biol. Chem. *278*, 44832–44842.

Kang, F., Purich, D. L., and Southwick, F. S. (1999). Profilin promotes barbed-end actin filament assembly without lowering the critical concentration. J. Biol. Chem. *274*, 36963–36972.

Kim, Y.-W., Yamashita, A., Wear, M. A., Maéda, Y., and Cooper, J. A. (2004). Capping protein binding to actin in yeast: biochemical mechanism and physiological relevance. J. Cell Biol. *164*, 567–580.

Kobayashi, I., Kobayashi, Y., and Hardham, A. R. (1994). Dynamic reorganization of microtubules and microfilaments in flax cells during the resistance response to flax rust infection. Planta. *195*, 237–247.

Kobayashi, I., Kobayashi, Y., Yamaoka, N., and Kunoh, H. (1992). Recognition of a pathogen and a nonpathogen by barley coleoptile cells. III. Responses of microtubules and actin filaments in barley coleoptile cells to penetration attempts. Can. J. Bot. *70*, 1815–1823.

Kouyama, T., and Mihashi, K. (1981). Fluorimetry study of *N*-(1-pyrenyl) iodoacetamide-labeled F-actin. Eur. J. Biochem. *114*, 33–38.

Kumar, N., Zhao, P. L., Tomar, A., Galea, C. A., and Khurana, S. (2004). Association of villin with phosphatidylinositol 4,5-bisphosphate regulates the actin cytoskeleton. J. Biol. Chem. *279*, 3096–3110.

Kusner, D. J., Barton, J. A., Qin, C., Wang, X., and Iyer, S. S. (2003). Evolutionary conservation of physical and functional interactions between phospholipase D and actin. Arch Biochem. Biophys. *412*, 231–241.

Kusner, D. J., Barton, J. A., Wen, K.-K., Wang, X., Rubenstein, P. A., and Iyer, S. S. (2002). Regulation of phospholipase D activity by actin. Actin exerts bidirectional modulation of mammalian phospholipase D activity in a polymerization-dependent, isoform-specific manner. J. Biol. Chem. *277*, 50683–50692.

Lassing, I., and Lindberg, U. (1985). Specific interaction between phosphatidylinositol 4,5-bisphosphate and profilactin. Nature *314*, 472–474.

Lee, S., Park, J., and Lee, Y. (2003). Phosphatidic acid induces actin polymerization by activating protein kinases in soybean cells. Mol. Cells *15*, 313–319.

Lee, S., Park, J. B., Kim, J. H., Kim, Y., Shin, K.-J., Lee, J. S., Ha, S. H., Suh, P.-G., and Ryu, S. H. (2001). Actin directly interacts with phospholipase D, inhibiting its activity. J. Biol. Chem. *276*, 28252–28260.

Li, W., Li, M., Zhang, W., Welti, R., and Wang, X. (2004). The plasma membrane-bound phospholipase Dδ enhances freezing tolerance in *Arabidopsis thaliana.* Nature Biotech. *24*, 427–433.

Lin, K.-M., Wenegieme, E., Lu, P.-J., Chen, C.-S., and Yin, H. L. (1997). Gelsolin binding to phosphatidylinositol 4,5-bisphosphate is modulated by calcium and pH. J. Biol. Chem. *272*, 20443–20450.

Loewen, C. J. R., Gaspar, M. L., Jesch, S. A., Delon, C., Ktistakis, N. T., Henry, S. A., and Levine, T. P. (2004). Phospholipid metabolism regulated by a transcription factor sensing phosphatidic acid. Science *304*, 1644–1647.

Lu, P.-J., Shieh, W.-R., Rhee, S. G., Yin, H. L., and Chen, C.-S. (1996). Lipid products of phosphoinositide 3-kinase bind human profilin with high affinity. Biochemistry *35*, 14027–14034.

Meerschaert, K., De Corte, V., De Ville, Y., Vandekerckhove, J., and Gettemans, J. (1998). Gelsolin and functionally similar actin-binding proteins are regulated by lysophosphatidic acid. EMBO J. *17*, 5923–5932.

Meijer, H. J. G., and Munnik, T. (2003). Phospholipid-based signaling in plants. Annu. Rev. Plant Biol. *54*, 265–306.

Miller, D. D., de Ruijter, N. C. A., Bisseling, T., and Emons, A. M. C. (1999). The role of actin in root hair morphogenesis: studies with lipochito-oligosaccharide as a growth stimulator and cytochalasin as an actin perturbing drug. Plant J. *17*, 141–154.

Monteiro, D., Liu, Q., Lisboa, S., Scherer, G. E. F., Quader, H., and Malhó, R. (2005a). Phosphoinositides and phosphatidic acid regulate pollen tube growth and reorientation through modulation of $[Ca^{2+}]_c$ and membrane secretion. J. Exp. Bot. *416*, 1665–1674.

Monteiro, D., Castanho Coelho, P., Rodrigues, C., Camacho, L., Quader, H., and Malhó, R. (2005b). Modulation of endocytosis in pollen tube growth by phosphoinositides and phospholipids. Protoplasma *226*, 31–38.

Ohashi, Y., Oka, A., Rodrigues-Pousada, R., Possenti, M., Ruberti, I., Morelli, G., and Aoyama, T. (2003). Modulation of phospholipid signaling by GLABRA2 in root-hair pattern formation. Science *300*, 1427–1430.

Pollard, T. D. (1984). Polymerization of ADP-actin. J. Cell Biol. *99*, 769–777.

Pollard, T. D., and Cooper, J. A. (1984). Quantitative analysis of the effect of *Acanthamoeba* profilin on actin filament nucleation and elongation. Biochemistry *23*, 6631–6641.

Potocký, M., Eliáš, M., Profotová, B., Novotná, Z., Vantová, O., and Žárský, V. (2003). Phosphatidic acid produced by phospholipase D is required for tobacco pollen tube growth. Planta *217*, 122–130.

Rizzo, M. A., Shome, K., Watkins, S. C., and Romero, G. (2000). The recruitment of Raf-1 to membranes is mediated by direct interaction with phosphatidic acid and is independent of association with Ras. J. Biol. Chem. *275*, 23911–23918.

Samaj, J., Baluska, F., and Menzel, D. (2004). New signalling molecules regulating root hair tip growth. Trends Plant Sci. *9*, 217–220.

Schafer, D. A., Jennings, P. B., and Cooper, J. A. (1996). Dynamics of capping protein and actin assembly in vitro: uncapping barbed ends by polyphosphoinositides. J. Cell Biol. *135*, 169–179.

Shin, I., Kweon, S.-M., Lee, Z.-W., Kim, S. I., Joe, C. O., Kim, J.-H., Park, Y.-M., and Ha, K.-S. (1999). Lysophosphatidic acid increases intracellular H$_2$O$_2$ by phospholipase D and RhoA in rat-2 fibroblasts. Mol. Cells *9*, 292–299.

Siddiqui, R. A., and English, D. (1997). Phosphatidic acid elicits calcium mobilization and actin polymerization through a tyrosine kinase-dependent process in human neutrophils: a mechanism for induction of chemotaxis. Biochim. Biophys. Acta *1349*, 81–95.

Sizonenko, G.I., Karpova, T. S., Gattermeir, D. J., and Cooper, J. A. (1996). Mutational analysis of capping protein function in *Saccharomyces cerevisiae*. Mol. Biol. Cell *7*, 1–15.

Snowman, B. N., Kovar, D. R., Shevchenko, G., Franklin-Tong, V. E., and Staiger, C. J. (2002). Signal-mediated depolymerization of actin in pollen during the self-incompatibility response. Plant Cell *14*, 2613–2626.

Staiger, C. J. (2000). Signaling to the actin cytoskeleton in plants. Annu. Rev. Plant Physiol. Plant Mol. Biol. *51*, 257–288.

Staiger, C. J., and Hussey, P. J. (2004). Actin and actin-modulating proteins. In: The Plant Cytoskeleton in Cell Differentiation and Development, ed. P. J. Hussey, Oxford, United Kingdom: Blackwell Publishers, 32–80.

Stinson, R. A., and Holbrook, J. J. (1973). Equilibrium binding of nicotinamide nucleotides to lactate dehydrogenases. Biochem. J. *131*, 719–728.

Testerink, C., Dekker, H. L., Lim, Z.-Y., Johns, M. K., Holmes, A. B., de Koster, C. G., Ktistakis, N. T., and Munnik, T. (2004). Isolation and identification of phosphatidic acid targets from plants. Plant J. *39*, 527–536.

Testerink, C., and Munnik, T. (2005). Phosphatidic acid: a multifunctional stress signaling lipid in plants. Trends Plant Sci. *10*, 368–375.

Vidali, L., McKenna, S. T., and Hepler, P. K. (2001). Actin polymerization is essential for pollen tube growth. Mol. Biol. Cell *12*, 2534–2545.

Wang, H.-Y., Yu, Y., Chen, Z.-L., and Xia, G.-X. (2005). Functional characterization of *Gossypium hirsutum* profilin 1 gene (*GhPFN1*) in tobacco suspension cells. Planta *222*, 594–603.

Wang, X. (2004). Lipid signaling. Curr. Opin. Plant Biol. *7*, 329–336.

Ward, L. D. (1985). Measurement of ligand binding to proteins by fluorescence spectroscopy. Meth. Enzymol. *117*, 400–414.

Wear, M. A., and Cooper, J. A. (2004a). Capping protein binding to S100B: implications for the "tentacle" model for capping the actin filament barbed end. J. Biol. Chem. *279*, 14382–14390.

Wear, M. A., and Cooper, J. A. (2004b). Capping protein: new insights into mechanism and regulation. Trends Biochem. Sci. *29*, 418–428.

Wear, M. A., Yamashita, A., Kim, K., Maéda, Y., and Cooper, J. A. (2003). How capping protein binds the barbed end of the actin filament. Curr. Biol. *13*, 1531–1537.

Yamashita, A., Maeda, K., and Maéda, Y. (2003). Crystal structure of CapZ: structural basis for actin filament barbed end capping. EMBO J. *22*, 1529–1538.

Yin, H. L., and Janmey, P. A. (2003). Phosphoinositide regulation of the actin cytoskeleton. Annu. Rev. Physiol. *65*, 761–789.

Zhang, W., Qin, C., Zhao, J., and Wang, X. (2004). Phospholipase Dα1-derived phosphatidic acid interacts with ABI1 phosphatase 2C and regulates abscisic acid signaling. Proc. Natl. Acad. Sci. USA *101*, 9508–9513.

Zhou, D., Luini, W., Bernasconi, S., Diomede, L., Salmona, M., Mantovani, A., and Sozzani, S. (1995). Phosphatidic acid and lysophosphatidic acid induce haptotactic migration of human monocytes. J. Biol. Chem. *270*, 25549–25556.

Zimmerle, C. T., and Frieden, C. (1989). Analysis of progress curves by simulations generated by numerical integration. Biochem. J. *258*, 381–387.

Zonia, L., and Munnik, T. (2004). Osmotically induced cell swelling versus cell shrinking elicits specific changes in phospholipid signals in tobacco pollen tubes. Plant Physiol. *134*, 813–823.